



Dielectric relaxation behavior of colloidal suspensions of palladium nanoparticle chains dispersed in PVP/EG solution

Zhen Chen, Kong-Shuang Zhao, Lin Guo, and Cai-Hong Feng

Citation: *The Journal of Chemical Physics* **126**, 164505 (2007); doi: 10.1063/1.2721561

View online: <http://dx.doi.org/10.1063/1.2721561>

View Table of Contents: <http://scitation.aip.org/content/aip/journal/jcp/126/16?ver=pdfcov>

Published by the [AIP Publishing](#)

Articles you may be interested in

[Electric-field induced phase transitions of dielectric colloids: Impact of multiparticle effects](#)

J. Appl. Phys. **111**, 094106 (2012); 10.1063/1.4714550

[Effect of stagnant-layer conductivity on the electric permittivity of concentrated colloidal suspensions](#)

J. Chem. Phys. **126**, 104903 (2007); 10.1063/1.2538679

[Theory of dielectrophoresis in colloidal suspensions](#)

J. Appl. Phys. **95**, 8321 (2004); 10.1063/1.1737050

[Nonlinear alternating current response of colloidal suspension with an intrinsic dispersion](#)

J. Appl. Phys. **93**, 2871 (2003); 10.1063/1.1543637

[Phase separation in suspensions of colloids, polymers and nanoparticles: Role of solvent quality, physical mesh, and nonlocal entropic repulsion](#)

J. Chem. Phys. **118**, 3880 (2003); 10.1063/1.1538600

A small image of the cover of an Applied Physics Reviews journal issue. It features a grid of colored squares and some text, with the AIP logo and 'Applied Physics Reviews' title at the top.

NEW Special Topic Sections

NOW ONLINE
Lithium Niobate Properties and Applications:
Reviews of Emerging Trends

AIP Applied Physics
Reviews

Dielectric relaxation behavior of colloidal suspensions of palladium nanoparticle chains dispersed in PVP/EG solution

Zhen Chen and Kong-Shuang Zhao^{a)}

College of Chemistry, Beijing Normal University, Beijing 100875, People's Republic of China

Lin Guo and Cai-Hong Feng

School of Materials Science and Technology, Beijing University of Aeronautics and Astronautics, Beijing 100083, People's Republic of China

(Received 5 January 2007; accepted 9 March 2007; published online 25 April 2007)

Dielectric measurements were carried out on colloidal suspensions of palladium nanoparticle chains dispersed in poly(vinyl pyrrolidone)/ethylene glycol (PVP/EG) solution with different particle volume fractions, and dielectric relaxation with relaxation time distribution and small relaxation amplitude was observed in the frequency range from 10^5 to 10^7 Hz. By means of the method based on logarithmic derivative of the dielectric constant and a numerical Kramers-Kronig transform method, two dielectric relaxations were confirmed and dielectric parameters were determined from the dielectric spectra. The dielectric parameters showed a strong dependence on the volume fraction of palladium nanoparticle chain. Through analyzing limiting conductivity at low frequency, the authors found the conductance percolation phenomenon of the suspensions, and the threshold volume fraction is about 0.18. It was concluded from analyzing the dielectric parameters that the high frequency dielectric relaxation results from interfacial polarization and the low frequency dielectric relaxation is a consequence of counterion polarization. They also found that the dispersion state of the palladium nanoparticle chain in PVP/EG solution is dependent on the particle volume fraction, and this may shed some light on a better application of this kind of materials. © 2007 American Institute of Physics. [DOI: [10.1063/1.2721561](https://doi.org/10.1063/1.2721561)]

I. INTRODUCTION

Metallic or inorganic nanoparticle (NP) assemblies have been intensively investigated in recent years, not only because they can yield collective physicochemical properties that are evidently different from single NPs as a result of their specific particle size, spacing, and organized structure,¹⁻³ but also because of their potential applications in electronic and photonic devices, telecommunications, and sensors.⁴ Tremendous efforts have thus been devoted to the preparation of a variety of NP assemblies with different size and well-defined morphologies, for instance, see Refs. 5-7. Compared with the synthesis works, however, corresponding research works on the structural properties of these newly synthesized NP assemblies are far from enough, even though it is well known that the structural properties can sometimes remarkably influence their physical and chemical properties.^{8,9} Therefore, research works of this kind by means of various modern physical techniques are highly deserved to carry out nowadays, especially those on the structural properties of NP assemblies in environments similar to those they are working in, for example, dispersed in liquid solutions.

Among many modern physical techniques, dielectric relaxation spectroscopy (DRS) occupies a special and important place due to its outstanding sensitivity to the properties of the systems under investigation as well as a number of

other advantages.^{10,11} For the characterization of colloidal suspensions, DRS now has become one of the most effective methods due to both these advantages and the development in theory, experiment, and data treatment in the past several decades. The dielectric theories on Maxwell-Wagner (MW) polarization relaxation¹²⁻¹⁴ and counterion polarization relaxation,¹⁵⁻¹⁷ which are the most typical relaxation mechanisms for colloidal suspensions in the radio frequency range, and can offer rich information on particle dispersion state, charge diffusion, interfacial configuration, and so on.¹⁸⁻²¹ Data treatment methods such as the logarithmic derivative method^{22,23} and numerical Kramers-Kronig transform method²⁴ have been developed in the past decade, which can markedly increase the accuracy of the dielectric data processing. Since many applications, such as used as catalyzer, demand that NP assemblies be in the state of colloidal suspension, DRS investigations on their colloidal suspensions may offer information about their structure in their working state, and thus are hoped to reveal the working mechanism and to further their applications.

The suspensions under study in this paper are suspensions of Pd NP chain dispersed in poly(vinyl pyrrolidone)/ethylene glycol (PVP/EG) solution, where the dispersed particles are chainlike metallic nanosphere assemblies covered by PVP molecules. Pd NPs have been extensively used as one of the primary catalysts for many organic reactions,²⁵ and their catalytic power is definitely influenced by such properties as dispersion state and surface/volume ratio. On the other hand, the dispersed Pd NP chains are highly con-

^{a)}Author to whom correspondence should be addressed. Electronic mail: zhaoks@bnu.edu.cn

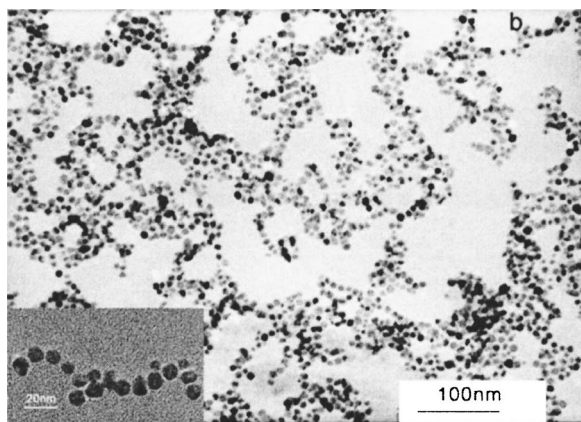


FIG. 1. Transmission electron microscope images of linear assemblies of Pd NP chains.

ducting particles with nonspherical shape and hence are much different from conventional dispersed particles previously investigated. Till now, experimental DRS investigations on conducting particle suspensions are fairly sparse to the best of our knowledge. Nevertheless, it will be shown in this paper that the basic principles of these theories are still applicable for such systems and DRS investigation on them can also provide important information on the dispersion state and surface/volume ratio of Pd NP chains in organic solutions. The result may help to facilitate the applications of Pd NP chains to fields such as catalysis and waste-water treatment on one hand, and may offer valuable evidence for the development of DRS theory on conducting particle suspensions on the other.

II. EXPERIMENT AND METHODS

A. Suspensions of Pd nanoparticle chain dispersed in PVP/EG solution

The one step polyol synthesis approach recently proposed by Feng *et al.*⁷ was used to produce short ordered Pd NP chains formed by using PVP as soft template. As can be seen from the transmission electron microscope picture (Fig. 1), The mean size of the particles in the Pd NP chains is about 8 nm, the interparticle distance is about 1.4 ± 0.6 nm, and the Pd NPs self-assemble to linear chain over 100 nm.

After the reaction was completed, the original reaction mixture, which is a mixture of Pd NP chains dispersed in PVP/EG solution with some inorganic ions, was used as mother suspension. Equal volume (0.5 ml) of mother suspensions were diluted by EG to 1, 2, 3, 4, 5, 6, 7, and 8 mL respectively. In this way, suspensions with different Pd NP chain volume fractions were obtained. Dielectric measurements were then carried out on these suspensions including the mother suspension without further treatments. The background PVP/EG solution at the absence of Pd NP chain was also conducted, which contains equivalent components to those of the mother suspension. Then the solution was diluted in the same way so as to obtain solutions with different PVP and inorganic ion concentration, and these solutions were conducted to dielectric measurements as well.

Since almost all Pd(II) can be reduced to Pd(0) after this

synthesis approach,⁷ the volume fraction ϕ of Pd NP chain of the mother suspension thus can be roughly estimated using the following formula:

$$\phi = \frac{M[\text{Pd(II)}]}{\rho}, \quad (1)$$

where [Pd(II)] is the initial Pd mole concentration, ρ is the Pd bulk density and M is the Pd molecular weight. According to the value of [Pd(II)] reported in Ref. 7, the volume fraction of the mother suspension is about 0.319, and the volume fractions of other suspensions under study are thus ranging from 0.02 to 0.159.

B. Dielectric measurement

Dielectric measurements were carried out using 4294A precise impedance analyzer (Agilent Technologies) controlled by a personal computer. The experiments were carried out at 25 ± 0.5 °C. The dielectric cell used in our study consists of concentric cylindrical platinum electrodes,²⁶ and the cell constant C_l and stray capacitance C_r that have been determined by use of several standard liquids were 0.47 and 0.081 pF, respectively, by which the directly measured conductance G and capacitance C at each frequency were transferred to the corresponding conductivity κ and dielectric constant ϵ' in line with the following relations: $\kappa = G\epsilon_0/C_l$ and $\epsilon' = (C - C_r)/C_l$, where ϵ_0 is the permittivity of vacuum. Prior to the transformation, all experimental data were subjected to certain corrections²⁷ for the errors arising from residual inductance due to the cell assembly. First, the inductance L_r (0.14 nH here) of the dielectric cell was determined by use of standard KCl solutions with different concentrations and the relation $C = L_r G^2$. Then all values of G and C were subjected to modification through the following expressions:²⁷

$$G_S = \frac{G_X}{(1 + \omega^2 L_r C_X)^2 + (\omega L_r G_X)^2},$$

$$C_S = \frac{C_X(1 + \omega^2 L_r C_X) + L_r G_X^2}{(1 + \omega^2 L_r C_X)^2 + (\omega L_r G_X)^2} - C_r,$$

where the subscript X and S denote the directly measured and modified values, respectively, and ω is the angular frequency.

C. Data treatment methods

1. Calculating dielectric loss from dielectric constant

Although dielectric loss (ϵ'') and dielectric constant (ϵ') are interrelated by the Kramers-Kronig relations, ϵ'' spectra often show more details and are therefore more suitable for the evaluation of complicated dielectric data than ϵ' spectra. Two methods were used here to calculate ϵ'' from ϵ' , both based on the Kramers-Kronig relations.

One is based on the analysis of the logarithmic derivative (LD) of dielectric constant,^{22,23} which is based on the following derivative:

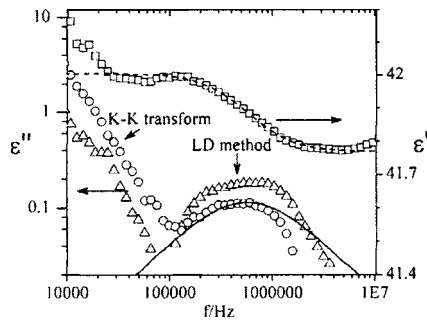


FIG. 2. Frequency dependences of dielectric constant (\square) and dielectric loss [LD method (Δ), K-K transform method (\circ)] of Pd NP chain suspension. The dashed line is fitting curve and solid line is theoretical curve.

$$\varepsilon''_{\text{Der}}(\omega) = -\frac{\pi}{2} \frac{\partial \varepsilon'}{\partial \ln \omega} \approx \varepsilon'_{\text{Rel}}(\omega), \quad (2)$$

where $\varepsilon''_{\text{Der}}$ and $\varepsilon''_{\text{Rel}}$ denote the derivative and real dielectric losses, respectively. This method is convenient and effective in eliminating electrode polarization effect, as shown in Refs. 19 and 23, it also offers a better way to resolve overlapping peaks due to its peak sharpening.²³

The other one is the numerical Kramers-Kronig transform method developed by Steeman,²⁴ which can be used to better analyze Ohmic conduction processes and relaxation processes. The basic idea of this method is to calculate the dielectric loss by weighted differences of dielectric constant data, by use of the following approximation: for central frequency ε' data,

$$\varepsilon''(\omega) \approx \sum_{i=1}^n b_i [\varepsilon'(\omega/2^i) - \varepsilon'(\omega 2^i)], \quad (3)$$

for lower edge frequency ε' data,

$$\begin{aligned} \varepsilon''(\omega) \approx & \sum_{i=1}^{n_{\text{Max}}} b_i [\varepsilon'(\omega/2^i) - \varepsilon'(\omega 2^i)] \\ & + \sum_{i=n_{\text{max}}+1}^4 b_i [\varepsilon'(\omega) - \varepsilon'(\omega 2^i)], \end{aligned} \quad (4)$$

and for higher edge frequency ε' data,

$$\begin{aligned} \varepsilon(\omega) \approx & \sum_{i=1}^{n_{\text{max}}} b_i [\varepsilon'(\omega/2^i) - \varepsilon'(\omega 2^i)] \\ & + \sum_{i=n_{\text{max}}+1}^4 b_i [\varepsilon'(\omega/2^i) - \varepsilon'(\omega)], \end{aligned} \quad (5)$$

The b_i ($i=1, 2, 3, 4$) coefficients for the calculation are listed in Ref. 24. To get a more accurate dielectric loss data, the dielectric constant data were measured over the frequency ranging from $2^{5.4}$ to $2^{26.6}$ Hz with an interval of 0.2 on the $\log_2 f$ ($f=\omega/2\pi$) scale. Although the first and the last four data could not be calculated in this way, this did not matter because no relaxations happened in the edge regions in this study.

As an example, Fig. 2 shows us the calculated dielectric loss of one of the suspensions by means of the above-mentioned two methods. It can be seen that, although the

results obtained from different methods are not exactly consistent with each other, they both show a wide relaxation distribution in the same frequency range, namely, 10^5 – 10^7 Hz. The dielectric loss curve derived from LD method is sharper, from which we can see that there are two mechanisms of dielectric relaxations contributing to the current dielectric behavior in this frequency range.

2. Determination of dielectric parameters from dielectric spectra

Now that two dielectric relaxations were observed, as shown in Fig. 2, the dielectric parameters can be determined by fitting the following Cole-Cole equation²⁸ with two Cole-Cole terms to experimental and calculated dielectric spectra:

$$\varepsilon'' = \varepsilon_h + \frac{\varepsilon_l - \varepsilon_m}{1 + (j\omega\tau_l)^{\beta_1}} + \frac{\varepsilon_m - \varepsilon_h}{1 + (j\omega\tau_h)^{\beta_2}}, \quad (6)$$

where $\varepsilon^* = \varepsilon' - j\varepsilon''$ is the complex dielectric constant, τ is the characteristic relaxation time, β is the Cole-Cole parameter ($0 < \beta \leq 1$) denoting the width of the distribution of relaxation times, and $j^2 = -1$. The subscripts l , m , and h denote the low, medium, and high frequency limit values, respectively. To obtain the most accurate dielectric parameters, we started with fitting Eq. (6) to experimental ε' curve, and then the obtained dielectric parameters were used to get a theoretical ε'' curve, which was compared with the derived ε'' curves (from both methods). During this process, the optimized results were determined by the nonlinear least-squares method²² to minimize the sum of the residuals for the dielectric constant ε' and dielectric loss ε'' .

$$\chi = \sum_i [\varepsilon'_e(\omega_i) - \varepsilon'_t(\omega_i)]^2 + \sum_i [\varepsilon''_e(\omega_i) - \varepsilon''_t(\omega_i)]^2, \quad (7)$$

where χ is the sum of squares error estimate, the subscripts e and t , respectively, refer to the experimental and theoretical values, and ω_i is i th angular frequency.

During the fitting process we found that the best fitting was only reached under the condition of having simultaneously $\beta_1=1$ and $\beta_2=1$. This means that the two relaxations are both of Debye type, and thereby implies that only two dielectric relaxations were involved in this frequency range, which is consistent with what was observed in the ε'' curve derived by LD method (see Fig. 2). The result shown in Fig. 2 also indicates clearly that the values of ε'' that calculated from numerical Kramers-Kronig (K-K) transform are more approximating to theoretical values; however, the LD method is definitely in favor of resolving overlapping relaxation peaks due to its peak sharpening. Therefore in the data treatment process hereinafter, LD method was used to find out characteristic relaxation frequency, and K-K transform method was used to determine dielectric parameters.

III. RESULTS AND DISCUSSION

Figure 3(A) shows us the frequency dependency of dielectric constant of Pd NP chain suspensions with different volume fractions, from which we can see that no dielectric relaxation can be observed for the mother suspension ($\phi=0.319$), but all the other suspensions with lower volume

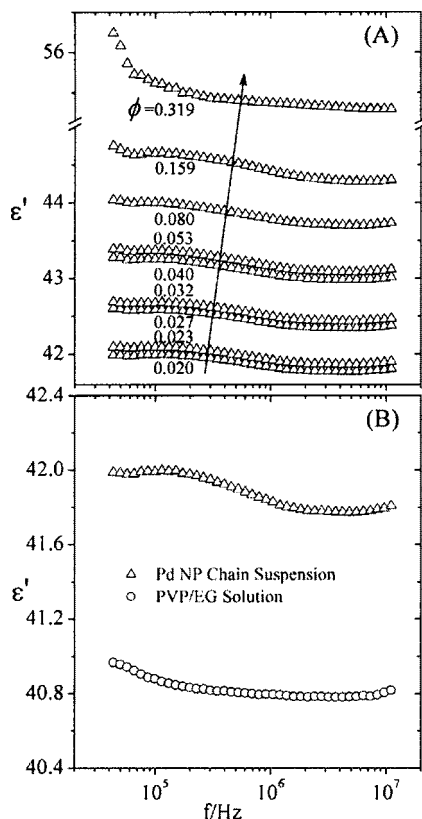


FIG. 3. Frequency dependences of dielectric constant of Pd NP chain suspensions with different volume fractions (A), and a comparison between the frequency dependency of dielectric constant of the suspension with $\phi=0.02$ and that of its corresponding PVP/EG solution as an example (B).

fractions distinctly exhibit dielectric relaxations in the frequency range from 10^5 to 10^7 Hz although the relaxation amplitudes are rather small. On the other hand, PVP/EG solutions also exhibit no dielectric relaxation in this frequency range, as shown in Fig. 3(B), where, as an example, the dielectric behavior of the Pd NP chain suspension with $\phi=0.02$ is compared with that of its corresponding PVP/EG solution. This definitely indicates that the dielectric relaxations observed in Fig. 3(A) are due to the existence of Pd NP chain in these suspensions. Dielectric parameters were determined in the way described above, which were listed in Table I. As shown in Table I, the relaxation amplitude is rather small, but the dielectric increment $\delta\epsilon$ and relaxation

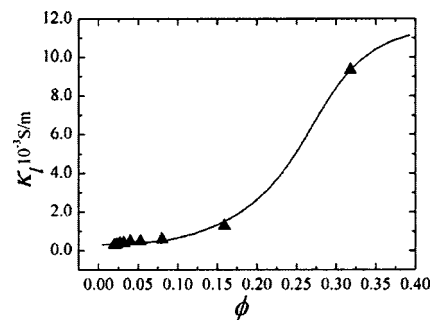


FIG. 4. Limiting conductivity at low frequency as a function of volume fraction for Pd NP chain suspensions. The line is drawn for guiding the eyes.

time of both low and high frequency dielectric relaxation vary regularly with increasing volume fraction.

The small relaxation amplitude is a characteristic of conducting or semiconducting particle suspensions.^{19,29} With respect to this phenomenon, Hanai²⁹ gave a phenomenological explanation aiming at water-in-oil-type emulsion and Dukhin and Shilov presented an electrokinetic analysis.³⁰ The fact that the mother suspension exhibits no relaxation in this frequency range is somewhat out of our expectation, which seems to imply that a special structure of the NP chains be formed when ϕ is bigger than a critical value.

A. The conductance percolation of Pd NP chain suspension

It is well known that the phenomenon of conductance percolation will occur in binary mixtures containing conductor and insulator such as the present systems.³¹ After a threshold volume fraction ϕ_t ($\phi_t \approx 0.17$) of spherical particles, the conductance increases sharply and then levels off. Basically, dielectric measurements can simultaneously give information on dielectric constant and conductivity of the systems under measurement. The limiting conductivity at low frequency κ_l is generally approximating to the dc conductivity of the system, which can be directly determined through fitting the conductivity spectra (listed in Table I). By plotting κ_l against the volume fraction of the Pd NP chain suspensions, we got Fig. 4, which demonstrates a typical conductance percolation behavior that the conductivity increases sharply when the volume fraction is about 0.18 and

TABLE I. Dielectric parameters of Pd NP chain suspensions dispersed in PVP/EG solution with different volume fractions. C_i is the concentration of the solution, τ is relaxation time, the subscripts l , m , and h denote the limiting value at low, medium, and high frequencies, and $\delta\epsilon_i = (\epsilon_i - \epsilon_m) / \phi$ and $\delta\epsilon_h = (\epsilon_m - \epsilon_h) / \phi$ represent low and high frequency dielectric increments, respectively.

ϕ	C_i (mol/m ³)	κ_l (mS/m)	ϵ'_l	ϵ'_m	ϵ'_h	τ_l (ns)	τ_h (ns)	$\delta\epsilon'_l$	$\delta\epsilon'_h$
0.020	0.83	0.298	42.0	41.9	41.8	407	232	4.1	7.8
0.023	0.95	0.311	42.1	42.0	41.9	401	231	4.6	6.0
0.027	1.11	0.380	42.6	42.5	42.3	404	213	3.9	5.6
0.032	1.33	0.386	42.7	42.6	42.4	423	219	3.2	4.9
0.040	1.67	0.480	43.3	43.1	43.0	465	193	3.5	3.7
0.053	2.22	0.483	43.4	43.2	43.1	505	187	2.8	3.0
0.080	3.33	0.581	44.0	43.9	43.7	569	170	2.0	2.1
0.159	6.67	1.281	44.7	44.6	44.3	612	159	0.8	1.7
0.319 ^a	13.30	9.328

^aSuspension with $\phi=0.319$ exhibits no dielectric relaxations.

then levels off at about 0.35. Therefore, from this figure we can find that the threshold volume fraction is about 0.18, which is approximating to 0.17 predicted by percolation theory.³¹ This also suggests that the values of ϕ calculated from Eq. (1) are reasonable. When $\phi < \phi_t$, we can imagine that most Pd NP chains are isolated although some chains may partially congregate; while when $\phi > \phi_t$, it is believed that a complex metallic matrix would be formed because of aggregation or some other mechanisms, and ion transfer channels would probably exist between the aggregated Pd NP chains, resulting in a sharp increase of conductivity. This may also account for the fact why no dielectric relaxations were observed for the mother suspension where $\phi > \phi_t$. In what follows, since the mother suspension exhibit no dielectric relaxations, it will no longer be considered in the discussion of the dielectric behaviors.

B. The mechanisms of high and low frequency dielectric relaxations

Few dielectric investigations are carried out on conducting particle suspensions, and discussions on the dielectric relaxation mechanisms of this kind of systems are rather rare to date. For the present suspension, which consists of relatively complicated compositions, a lot of relaxation mechanisms may contribute to the observed dielectric relaxations. One of these possibilities is the rotation of PVP molecules, however, as previously discussed, since no relaxations are observed in background PVP/EG solution, this possibility can be ruled out and the dielectric relaxations are surely due to the existence of Pd NP chain. The most likely mechanisms that immediately comes to mind are MW polarization¹²⁻¹⁴ and counterion polarization.¹⁵⁻¹⁷ The former is due to the buildup of charge on the interface at the presence of an applied electrical field, and the latter mainly arises from a field induced polarization of electrical double layer (EDL) where counterion prevails.

Essentially, characteristic relaxation time (τ) is the most effective criterion for confirming the mechanism of a dielectric relaxation. For MW polarization relaxation, its time scale corresponds to a charge carrier diffusing a distance of the order of the Debye length or double layer thickness κ^{-1} ,³²

$$\kappa^{-1} = \sqrt{\frac{\epsilon_a \epsilon_0 K T}{e^2 \sum_i C_i Z_i^2}}, \quad (8)$$

here K , T , C_i , and Z_i are Boltzmann constant, absolute temperature, number concentration of free charge, and valence of type i ions, respectively, ϵ_a is the permittivity of the electrolyte solution. For the present suspensions, although the disperse medium is not an aqueous solution, Eq. (8) is still applicable because the dielectric constant of EG is large enough to support an EDL and because the electrokinetic behavior of the suspensions is analogous to that observed in aqueous systems.³³ On the other hand, the dispersed particles in the present case are conducting metallic particles, so the field lines are locally perpendicular rather than parallel to the surface of the particle in an applied electric field, which means tangential movement of counterions along the surface, and hence the surface conductivity, is negligible.³⁴ The MW

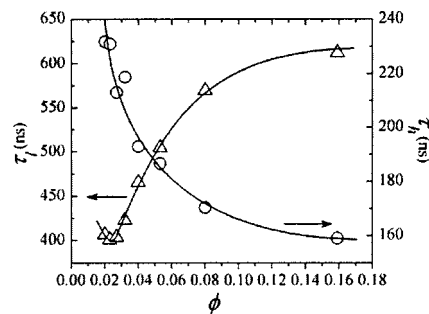


FIG. 5. Volume fraction dependency of the relaxation time of low (▲) and high (●) frequency dielectric relaxations of Pd NP chain suspension. The real lines are drawn for guiding the eyes.

polarization relaxation time, accordingly, can be more accurately estimated by the well-known Einstein equation, that is

$$\tau_{MW} = \kappa^{-2} / D_{MW}, \quad (9)$$

where D_{MW} is the ion diffusion coefficient in the region where space charge built up. However, the polarization of conducting particles is different from that of insulating particles,^{30,34} and the τ_{MW} of conducting particle suspension thus is thought to be κa (a is the particle radius) times longer than that of insulating particle suspension, that is

$$\tau_{MW} = a \kappa^{-1} / D_{MW}. \quad (10)$$

The relaxation time of counterion polarization relaxation for a spherical particle, on the other hand, corresponds to the time for the counterion to diffuse from one side of the particle to the other.³⁵ This distance is of the order of $2(a + \kappa^{-1})$, therefore the counterion polarization relaxation time can be estimated by

$$\tau_C = \frac{4(a + \kappa^{-1})^2}{D_C}, \quad (11)$$

where D_C is the counterion diffusion coefficient.

Since the mother suspensions were diluted with EG (solvent) that does not include small inorganic ions such as Cl^- ions, the concentration of small inorganic ions (solute) decreases with the dilution of the mother suspension, and hence C_i decreases as the volume fraction decreases. The estimated values of C_i are listed in Table I, which were roughly calculated from the hydrochloric salt concentration reported in Ref. 7 and the dilution multiples. The values of κ^{-1} calculated from Eq. (8) thus range from 2.58 to 7.31 nm, which are comparable to the radius of Pd nanoparticle. Consequently, κ^{-1} could not be neglected from Eq. (11) as done in thin double layer systems where $\kappa a \gg 1$, and it is not difficult to conclude that τ_C is always bigger than τ_{MW} and that they should both decrease with an increasing C_i or ϕ . Now we can judge, for the moment, that the high frequency dielectric relaxation is attributed to MW polarization and the low frequency one is a result of counterion polarization.

Figure 5 shows us the volume fraction dependency of the relaxation times of low and high frequency relaxations, from which we can find that with increasing ϕ , τ_h decreases while τ_l increases. This obvious volume fraction dependency of the relaxation times is certain evidence that these dielectric relaxations arise from induced dipole moment instead of

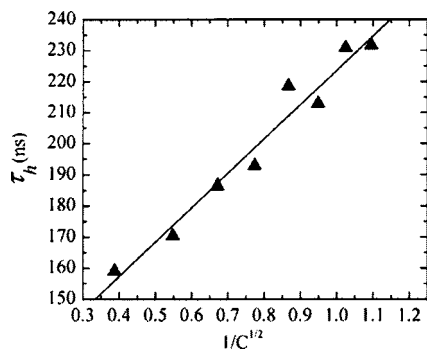


FIG. 6. Relaxation time of high frequency dielectric relaxation of Pd NP chain suspensions as a function of the reciprocal of the square root of the ionic concentration.

permanent dipole moment such as PVP molecule. The volume fraction dependency of τ_h is not beyond our expectation. In accordance with Eq. (10), τ_{MW} should linearly increase with increasing $C^{-1/2}$ considering that a and D_{MW} are constants. We plotted τ_h as a function of $C^{-1/2}$ in Fig. 6, in which the linear dependency surely consolidates the conclusion that the high frequency dielectric relaxation results from MW polarization. This linear dependency also signifies that MW polarization relaxation is somewhat independent of particle aggregation before the threshold volume fraction. In other words, despite the particle aggregation, the distance between the adjacent particles still keeps a characteristic distance of the order of κ^{-1} . By the slope of this linear dependency, D_{MW} can be calculated from Eq. (10), which is about $2.42 \times 10^{-10} \text{ m}^2/\text{s}$. This value is reasonable considering that the inorganic ions are solved in EG whose viscosity is one order bigger than that of water.

The low frequency dielectric relaxation thus should be attributed to counterion polarization. Nevertheless, it should be noted that two counterion polarization relaxations are supposed to be observed due to the chainlike configuration of the Pd NP assemblies in principle, which correspond to the diffusion of counterions parallel and perpendicular to the NP chain, respectively. The relaxation time of the relaxation arising from the parallel diffusion of counterions basically falls into the frequency range far beyond the frequency region of interest, because the length of the Pd NP chain here is over 100 nm. Accordingly, the low frequency dielectric relaxation observed in Fig. 3 is a result of the perpendicular diffusion of counterions, and the relaxation time is equivalent to that of single spherical particle, i.e., consistent with Eq. (11). The volume fraction dependency of τ_l , as shown in Fig. 5, was surprising to us because it is not in line with the prediction of Eq. (11) and also deviates from the prediction of the dielectric theory of concentrated dispersion proposed by Carrique *et al.*³⁶ The theory predicts that the characteristic time for the low frequency relaxation τ_l decreases with the increasing volume fraction, because the diffusion length of the counterion around the particle will be reduced by the presence of the neighboring particles as the volume fraction increases. For the present case, however, the dispersed particles are chain-like and easy to distort, therefore the result shown in Fig. 5 seems to indicate that the dispersion state of the Pd NP chain is varying with the volume fraction.

C. The dispersion state of palladium nanoparticle chain in the PVP/EG solution with different volume fractions

When ϕ is smaller than 0.03, we can find from Fig. 5 that τ_l is barely changed and even has a minor decrease with the increasing ϕ , which is normal according to Eq. (11). Under this condition, it is believed that the Pd NP chains are fully stretching and no interaction exists among them. The value of D_C calculated from Eq. (11) is about $8.35 \times 10^{-10} \text{ m}^2/\text{s}$, which is bigger than that of D_{MW} although both are of the same order. This is not surprising taking into account the following fact. On one hand, the Pd NP is surrounded by PVP molecules, which are absorbed by the surface via the coordination of the PVP carbonyl group to the Pd atoms,^{38,39} therefore the diffusion of the ions within the double layer is blocked by PVP molecules and is slower than in bulk solution. On the other hand, since tangential counterion diffusion around the particle is forbidden as previously discussed, the volume diffusion mechanism proposed by Dukhin and Shilov¹⁶ is preferable to account for the present dielectric relaxation, that is, the relaxation arises from the diffusion of ions in the bulk solution adjoining the EDL due to a concentration gradient, and D_C is comparable to that in bulk solution.

Whereas when ϕ is bigger than 0.03, τ_l increases obviously with the increasing ϕ . This phenomenon seems to suggest that the Pd NP chain begins to fold and then to aggregate when $\phi > 0.03$. It should be kept in mind that the Pd NP chains are covered by a PVP shell and the EDL around the chain is comparable thick, which means the chains actually occupy much more volume than that of naked chains. Therefore, even at not very high volume fraction, an increase in ϕ will bring about a potential electrostatic repulsion between the adjoining chains. To ease this electrostatic repulsion, it is likely that the chain will contract itself and form a folded chain, as shown in the inset of Fig. 1. This will then result in a longer time for counterions to diffuse from one side of the chain to the other, and hence a bigger τ_l . The contraction, however, will not continue forever, so a further increase in ϕ will give rise to aggregation and thus an increasing τ_l . Judged from the curves in Fig. 5, the watershed volume fraction from contraction to aggregation seems to be around 0.08.

The dispersion state of Pd NP chain may also be reflected by the volume fraction dependency of dielectric increments. Figure 7 gives us the volume fraction dependency of the dielectric increments of low and high frequency dielectric relaxations of Pd NP chain suspensions, where $\delta\epsilon_l = (\epsilon_l - \epsilon_m)/\phi$ and $\delta\epsilon_h = (\epsilon_h - \epsilon_m)/\phi$. From this figure we can tell that both $\delta\epsilon_l$ and $\delta\epsilon_h$ are decreasing with increasing ϕ , which is consistent with the prediction of the theory of Carrique *et al.*,³⁶ but the decreases distinctly trail off after ϕ is about 0.08. This result thus also indicates that the aggregation happens when the volume fraction is bigger than 0.08. It is well known that relaxation amplitude, for example, $\Delta\epsilon_l (= \epsilon_l - \epsilon_m)$, increases with increasing volume fraction,³⁵⁻³⁷ but dielectric increment denotes the relaxation amplitude per unit volume and thereby is only decided by the induced dipole coefficient of a single particle. As the volume fraction

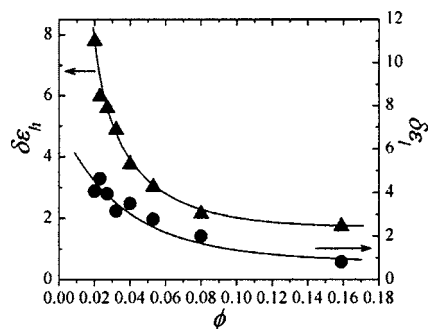


FIG. 7. Volume fraction dependency of the dielectric increments of low (●) and high (▲) frequency dielectric relaxations of Pd NP chain suspensions. Real lines are for guiding the eyes.

increases, ion concentration in the bulk solution increases, then more counterions will reside in the stagnant layer of EDL and fewer counterions will be left in the diffuse layer. As concluded from several former works,^{20,21} the dielectric increment of MW polarization relaxation for conducting particles is mainly a function of the counterion concentration in the diffuse layer, therefore $\delta\epsilon_h$ basically decreases with increasing ϕ . The fewer counterions in the diffuse layer, on the other hand, lead to a relatively smaller concentration gradient in the adjoining bulk solution, accordingly $\delta\epsilon_l$ also decreases with increasing ϕ . When aggregation happens, say $\phi > 0.08$, the interaction between the chains will definitely influence the counterion distribution of the EDL. At the presence of an applied field, it is not difficult to imagine that each chain is polarized with excess positive charges on one side and excess negative charges on the other, and for adjacent chains, the positively charged side of one chain will certainly face to the negatively charged side of the other chain. This situation is surely in favor of allowing some counterions that originally reside in the stagnant layer to go into the diffuse layer due to the electric attraction, so the dielectric increment of aggregated chains will not decrease as intensely as the single chain does.

Summarizing, when ϕ is smaller than the threshold volume fraction ϕ_t , since for conducting particles the surface potential will be held constant even when the charge density in the EDL changes,¹⁴ the volume fraction dependency of the dielectric increments, as shown in Fig. 7, apparently indicates that the surface/volume ratio of the Pd NP chains is reducing with the increasing volume fraction due to the folding or aggregation of the chains. Whereas when ϕ is bigger than ϕ_t , as previously discussed, a rather complex metallic matrix will be formed due to further aggregation, and ion transfer channels will exist between the aggregated Pd NP chains. Under this condition, MW polarization is likely to occur at a much higher frequency range because of the ion transfer channels, while counterion polarization will probably fall into a rather lower frequency range because more time is needed for counterions to diffuse over the metallic matrix.

IV. CONCLUDING REMARKS

In the frequency range from 10^5 to 10^7 Hz, dielectric relaxations with wide relaxation time distribution and small

relaxation amplitude were observed for the suspensions of Pd NP chain dispersed in PVP/EG solution with different volume fractions, which exhibited a distinct dependency on the volume fraction. Two relaxations were confirmed in this frequency range by means of the logarithmic derivative method, which turned out to be very effective in resolving overlapped relaxations. While it is found that the numerical Kramers-Kronig transform method is able to obtain dielectric loss more approximating to real values, by using which the dielectric parameters were accurately determined.

The low frequency limiting conductivity κ_l is dependent on the volume fraction, which shows a typical conductance percolation phenomenon of Pd NP chain suspension, with a threshold volume fraction of about 0.18. Through analyzing the volume fraction dependent relaxation time, we attributed the mechanisms of high and low frequency dielectric relaxations to Maxwell-Wagner polarization and counterion polarization, respectively. The volume fraction dependency of low frequency relaxation time as well as the dielectric increments disclosed a variation of dispersion state of the Pd NP chains with the increasing volume fraction. When the volume fraction is very low, the chains are totally isolated and fully stretched. As the volume fraction increases, the chains begin to contract and fold due to electrostatic repelling; and a further increase of the volume fraction, say, bigger than 0.08, will lead to local aggregation of the chains. While when the volume fraction is bigger than the threshold volume fraction, a metallic matrix seems to be formed from an overall aggregation of the chains and ion transfer channels seems to exist between them, resulting in not only a sharp increase of conductivity but also the absence of dielectric relaxation for the mother suspension.

This contribution is another evidence of the effectivity of dielectric relaxation spectroscopy on the characterization of the properties of constituent phases and their interface of colloidal suspensions, and the result is hoped to facilitate the application of Pd NP chain to catalysis and waste-water treatment.

ACKNOWLEDGMENT

Financial support of this work by the National Natural Science Foundation of China (Nos. 20673014 and 20673009) is gratefully acknowledged.

¹C. P. Collier, T. Vossmeier, and J. R. Heath, *Annu. Rev. Phys. Chem.* **49**, 371 (1998).

²M. P. Pileni, *J. Phys. Chem. B* **105**, 3358 (2001).

³B. Kim, S. L. Tripp, and A. Wei, *J. Am. Chem. Soc.* **123**, 7955 (2001).

⁴G. M. Whitesides, J. K. Kriebel, and B. T. Mayers, in *Nanoscale Assembly*, edited by W. T. S. Huck (Springer, New York, 2005), pp. 217–239.

⁵S. L. Tripp, S. V. Pusztay, A. E. Ribbe, and A. Wei, *J. Am. Chem. Soc.* **124**, 7914 (2002).

⁶C. M. Liu, L. Guo, R. M. Wang, Y. Deng, H. B. Xu, and S. Yang, *Chem. Commun. (Cambridge)* **2004**, 2726.

⁷C. H. Feng, Z. G. Shen, and L. Guo, *Chem. Phys. Lett.* (submitted); C. H. Feng, Ph.D. thesis, Beijing University of Aeronautics and Astronautics, 2007.

⁸J. Z. Zhang, *Acc. Chem. Res.* **30**, 423 (1997).

⁹J. S. Bradley, E. W. Hill, S. Behal, and C. Klein, *Chem. Mater.* **4**, 1234 (1992).

¹⁰F. Kremer and A. Schonhals, *Broadband Dielectric Spectroscopy* (Springer-Verlag, Berlin, 2002).

- ¹¹ F. Kremer, Dielectrics Newsletter, issue March 1994, p. 3.
- ¹² J. C. Maxwell, *A Treatise on Electricity and Magnetism*, 3rd ed. (Clarendon, Oxford, 1891).
- ¹³ K. W. Wagner, Arch. Elektrotech. (Berlin) **2**, 371 (1914).
- ¹⁴ S. S. Dukhin, Discuss. Faraday Soc. **51**, 158 (1971).
- ¹⁵ G. Schwarz, J. Phys. Chem. **66**, 2636 (1962); J. M. Schurr, *ibid.* **68**, 2407 (1964).
- ¹⁶ S. S. Dukhin and V. N. Shilov, *Dielectric Phenomena and the Double Layer in Disperse Systems and Polyelectrolytes* (Wiley, New York, 1974).
- ¹⁷ W. C. Chew and P. N. Sen, J. Chem. Phys. **77**, 4683 (1982).
- ¹⁸ M. L. Jiménez, F. J. Arroyo, F. Carrique, and U. Kaatz, J. Phys. Chem. B **107**, 12192 (2003).
- ¹⁹ Z. Chen and K. S. Zhao, J. Colloid Interface Sci. **276**, 85 (2004).
- ²⁰ K. S. Zhao and Z. Chen, Colloid Polym. Sci. **284**, 1147 (2006).
- ²¹ K. Asami, Langmuir **21**, 9032 (2005).
- ²² M. L. Jiménez, F. J. Arroyo, J. van Turnhout, and A. V. Delgado, J. Colloid Interface Sci. **249**, 327 (2002).
- ²³ M. Wübbenhorst and J. van Turnhout, J. Non-Cryst. Solids **305**, 40 (2002).
- ²⁴ P. A. M. Steeman and J. van Turnhout, Colloid Polym. Sci. **275**, 106 (1997).
- ²⁵ M. Moreno-manas and R. Pleixats, Acc. Chem. Res. **36**, 638 (2003).
- ²⁶ A. Ishikawa, T. Hanai, and N. Koizumi, Jpn. J. Appl. Phys. **20**, 79 (1981).
- ²⁷ K. Asami, A. Irimajiri, T. Hanai, and N. Koizumi, Bull. Inst. Chem. Res., Kyoto Univ. **51**, 231 (1973).
- ²⁸ K. S. Cole and R. H. Cole, J. Chem. Phys. **9**, 341 (1941).
- ²⁹ T. Hanai, *Emulsion Science*, edited by P. Sherman (Academic, London, 1968).
- ³⁰ S. S. Dukhin and V. N. Shilov, Adv. Colloid Interface Sci. **13**, 153 (1980).
- ³¹ D. Stauffer and A. Aharony, *Introduction to Percolation Theory* (Taylor and Francis, London, 1992).
- ³² S. S. Dukhin, Adv. Colloid Interface Sci. **61**, 17 (1995).
- ³³ Ph. C. Van der Hoeven and J. Lyklema, Adv. Colloid Interface Sci. **42**, 205 (1992).
- ³⁴ R. W. O'Brien, J. Colloid Interface Sci. **113**, 81 (1986).
- ³⁵ E. H. B. Delacey and L. R. White, J. Chem. Soc., Faraday Trans. 2 **77**, 2007 (1981).
- ³⁶ F. Carrique, F. J. Arroyo, M. L. Jimenez, and A. V. Delgado, J. Chem. Phys. **118**, 1945 (2003).
- ³⁷ V. N. Shilov, A. V. Delgado, F. Gonzalez-Caballero, and C. Grosse, Colloids Surf., A **192**, 253 (2001).
- ³⁸ T. Teranishi and M. Miyake, Chem. Mater. **10**, 594 (1998); G. Cardenas-Trivino, R. A. Segura, and J. Reyes-Gasga, Colloid Polym. Sci. **282**, 1206 (2004).
- ³⁹ A. Nemamcha, J. L. Rehspringer, and D. Khatmi, J. Phys. Chem. B **110**, 383 (2006).